PHASE RETRIEVAL FOR OPTICAL BEAMS WITH 1-DIMENSIONAL TRANSVERSE DOMAIN

Victor-Cristian Palea[1] and Liliana Preda[1]

We propose a method of computing the phase function for optical beams with 1-dimensional transverse space using amplitude data defined on multiple steps along the propagation axis. The computation is based on the propagation model of the wave equation in the paraxial approximation.

Keywords: phase retrieval, wave equation, paraxial approximation, amplitude profile, phase profile

1. Introduction

The computation of the phase function for optical beams is known as the phase retrieval problem[1] and has been addressed under various forms. Probably one of the most well known solutions to it is the Gerchberg-Saxton algorithm[2] which computes the phase corresponding to two amplitude profiles. Other similar algorithms have also been developed[3, 4], including extensions to three planes[5]. From an experimental perspective Shack-Hartmann sensors can be used to characterize an optical profile in terms of its phase[6, 7, 8], along with interferometric methods[9, 10] and aperture arrays[11].

Other methods that are more focused on the propagation model have also been proposed, as is the case of using the transport-of-intensity equation (TIE)[12, 13]. Solutions for the phase retrieval problem using TIE consist of using Zernike polynomials[14, 15] or Green's functions[13, 16]. These methods address the retrieval of the phase function on a transverse plane at a given position on the propagation axis, using measured amplitude data. This raised the possibility of extending the TIE approach from one profile to a finite propagation distance on which the amplitude is known.

We propose a solution for this phase retrieval problem, which in the following will be referred to as WBPR (whole beam phase retrieval). The method addresses the advantages and limitations of retrieving the phase function given amplitude data at multiple positions along the propagation axis for 1-dimensional transverse beams. The differences between TIE and WBPR

[1]Asistent, Faculty of Applied Sciences, University POLITEHNICA of Bucharest, Romania, e-mail: victor.palea@physics.pub.ro

[1]Lecturer, Faculty of Applied Sciences, University POLITEHNICA of Bucharest, Romania, e-mail: liliana.preda@physics.pub.ro

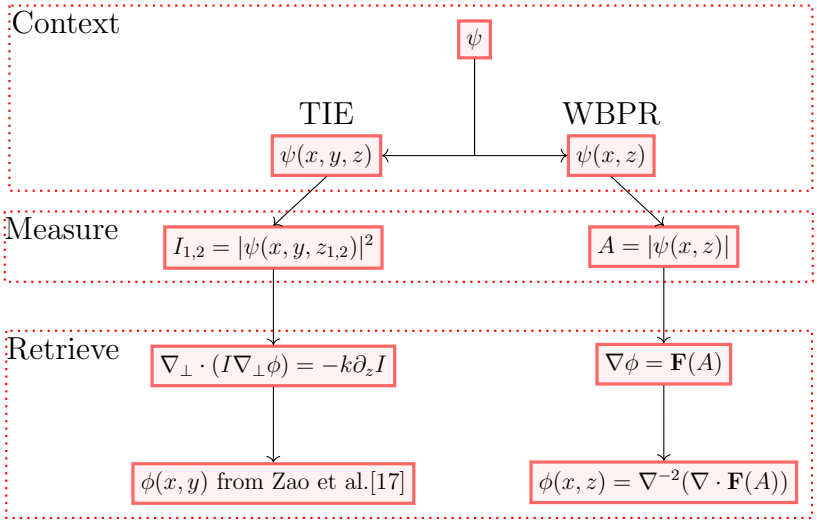

FIG. 1. Flow charts for the comparison between the TIE and WBPR methods for phase retrieval. ψ is the solution to the propagation equation, z is the propagation axis, x and y represent transverse axes, k is the wavenumber, $\nabla_\perp = (\partial_x, \partial_y)$, $\nabla = (\partial_x, \partial_z)$ for the WBPR case, $\mathbf{F}$ is a function that is presented in section 2.**2** and ϕ is the retrieved phase function.

are condensed in figure 1. Both TIE and WBPR aim at retrieving the phase function in order to obtain the complex valued solution of the propagation equation. The TIE method is usually considered for a two dimensional transverse domain (x, y), although Teague offered a solution of the 1-dimensional case also[12]. The intensity data is measured around the position of interest along the propagation axis, usually at two transverse planes z_1 and z_2 in order to numerically evaluate the term $\partial_z I$ from the retrieval step. This allows for the computation of the phase function $\phi(x, y)$ at $z = (z_1 + z_2)/2$ under various assumptions regarding the boundary conditions [17].

WBPR considers only a 1-dimensional transverse domains and uses amplitude data at multiple points (more than two) along the propagation axis. In short, while TIE uses the amplitude data in two planes in order to compute one in-between transverse phase profile, the WBPR approach uses multiple planes in order to compute multiple phase profiles for each plane at which amplitude data has been collected. The phase retrieval is done by inverting a Poisson type partial differential equation (PDE), thus generating the phase for the entire optical beam.

In this article we present the theoretical result on which WBPR is based, two implementations for solving the Poisson PDE from figure 1, and three numerical case studies, followed by an analysis of the advantages and limitations of the method.

2. Mathematical background for WBPR

In this section we present the derivation of the PDE used for retrieving the phase function and the two scenarios on which the retrieval is applied.

2.1. Deriving the retrieval PDE

The PDE that models the paraxial wave equation for the transverse 1-dimensional case is

$$\partial_z \psi = \frac{i}{2k} \partial_x^2 \psi \tag{1}$$

where k is the wavenumber and $\psi : \mathbb{R}^2 \to \mathbb{C}$ represents the slowly varying envelope of the electric field.

By substitution $\psi = A \exp(i\phi)$ equation (1) becomes

$$(\partial_z A + iA\partial_z \phi) = \frac{i}{2k}(\partial_x^2 A + 2i\partial_x A \partial_x \phi + iA\partial_x^2 \phi - A(\partial_x \phi)^2) \tag{2}$$

which can be split in two equations by identifying the real and imaginary parts of equation (2)

$$\partial_z A = -\frac{1}{2k}(2\partial_x A \partial_x \phi + A\partial_x^2 \phi) \tag{3}$$

$$A\partial_z \phi = \frac{1}{2k}(\partial_x^2 A - A(\partial_x \phi)^2). \tag{4}$$

Solving for $\partial_x \phi$ in equation (3) we get

$$\partial_x \phi = -\frac{k}{A^2} \partial_z \int_{x_0}^{x} A^2 dx' + \frac{(A^2 \partial_x \phi)|_{x=x_0}}{A^2}. \tag{5}$$

Introducing $\partial_x \phi$ from (5) in (4) gives

$$\partial_z \phi = \frac{1}{2kA} \left(\partial_x^2 A - A \left(\frac{k}{A^2} \partial_z \int_{x_0}^{x} A^2 dx' + \frac{(A^2 \partial_x \phi)|_{x=x_0}}{A^2} \right)^2 \right) \tag{6}$$

Theoretically, by solving equations (5) and (6) one can retrieve the phase function for the given amplitude function.

Equations (5-6) can be rewritten for simplicity as

$$\nabla \phi = \mathbf{F}. \tag{7}$$

where $\mathbf{F} : \mathbb{R}^2 \to \mathbb{R}^2$ is given by the right-hand side terms.

Since ϕ is a phase function, it is described by a scalar field. Then it is true that $\nabla \times (\nabla \phi) = 0$, which should be equivalent to $\nabla \times \mathbf{F} = 0$. This could be expected when the amplitude function is known to correspond to an actual optical beam, but it might not necessarily be the case if numerical or measurement errors exist in the amplitude data, so it is probable that for some cases $\nabla \times \mathbf{F} \neq 0$.

The implication is that the function $\mathbf{F}$ from equation (7) has a curl-free component and a divergence-free component such that

$$\mathbf{F} = \nabla\varphi_{div} + \nabla \times \boldsymbol{\varphi}_{curl} \tag{8}$$

according to the Helmholtz decomposition.

Since the desired phase function has to be a scalar field, based on equation (8) we assume that $\nabla \times \boldsymbol{\varphi}_{curl}$ has to be excluded from the computation. This can be achieved by applying the divergence $\nabla\cdot$ operator on equation (8) which gives

$$\nabla \cdot \mathbf{F} = \Delta\varphi_{div} + \nabla \cdot (\nabla \times \boldsymbol{\varphi}_{curl}) = \Delta\varphi_{div}. \tag{9}$$

because by definition $\nabla \cdot (\nabla \times \boldsymbol{\varphi}_{curl}) = 0$.

From equation (9) the term φ_{div} can be considered to be the desired phase function ϕ, such that equation (9) can be expressed as

$$\Delta\phi = \nabla \cdot \mathbf{F} \tag{10}$$

which is a Poisson equation and can be inverted formally[18] giving the solution

$$\phi = \Delta^{-1}(\nabla \cdot \mathbf{F}). \tag{11}$$

2.**2**. **Existence of background**

A particular scenario related to solving for the phase function can be obtained starting from equations (5-6). In the general case of equations (5-6) it is required that both $\partial_x\phi(x_0)$ is known and that $A \neq 0$. If however a spread out beam passes through a material that slightly changes the phase function, both issues can be avoided by considering solutions with a background level for which the amplitude function is given by $\bar{A} = |A\exp(i\phi) + c|$ where $c \in \mathbb{R}^*_+$ is a constant, such that $\bar{A} > 0$. In this case we can compute a vector field $\mathbf{F}$ given by equations (5) and (6) such that

$$\mathbf{F} = \begin{pmatrix} -\frac{k}{\bar{A}^2}\partial_z \int_{x_0}^{x} \bar{A}^2 dx' \\ \frac{1}{2k\bar{A}} \left(\partial_x^2 \bar{A} - \bar{A} \left(\frac{k}{\bar{A}^2}\partial_z \int_{x_0}^{x} \bar{A}^2 dx' \right)^2 \right) \end{pmatrix}. \tag{12}$$

where the term $\partial_x\phi(x_0)$ has been neglected. The addition of constant c implies that the function $\psi = R + iI$, where R is the real part and I is the imaginary part, becomes $\bar{\psi} = (R + c) + iI$ which translates to having the new amplitude function

$$\bar{A} = \sqrt{(R + c)^2 + I^2} = \sqrt{R^2 + I^2 + c^2 + 2Rc} = \sqrt{A^2 + c^2 + 2Rc} \tag{13}$$

where $A^2 = R^2 + I^2 = |\psi|^2$, while the new phase function becomes

$$\bar{\phi} = \operatorname{atan}\left(\frac{I}{R + c}\right). \tag{14}$$

We notice that if $c \gg \max(R)$, equations (13-14) can be approximated to $\bar{A} \to c$ and $\bar{\phi} \to 0$ which implies that the magnitude of the phase function

and its change along each variable is diminished

$$\lim_{c\to\infty} \partial_x \bar{\phi} = \lim_{c\to\infty} \frac{1}{1+\left(\frac{I}{R+c}\right)^2} \cdot \left(\frac{\partial_x I}{R+c} - \frac{I\partial_x R}{(R+c)^2}\right) = 0. \tag{15}$$

We however are interested in the regions where the initial amplitude would have tended to 0, i.e. the boundaries of the transverse spatial domain. The effect of having a background here assures that $\partial_x \phi(x_0) \to 0$ if x_0 is at the boundary of the domain.

This implies that from a practical perspective the background can be $c \approx \max(A)$ and the effect of reducing the influence of the initial condition is still satisfied, since in (15) $c \gg R$ and $c \gg I$ because $R \to 0$ and $I \to 0$ as $x \to x_0$.

3. Numerical implementation

Two methods have been used to solve equations (10-11) in order to exclude possible numerical artifacts due to a specific implementation of the numeric schemes.

3.1. Fourier Transform (FT)

The first method uses the Fourier Transform (FT with $\mathscr{F}$ symbol) of equation (11) which gave

$$\tilde{\phi} = \frac{-1}{4\pi^2(\xi^2+\eta^2)} \mathscr{F}\left[\nabla \cdot \mathbf{F}\right] \tag{16}$$

where ξ and η are the spatial frequencies associated with the x and z axes. Check the appendix for a complete derivation of 16.

Equation (16) can be evaluated numerically for a discrete amplitude function that is used to compute $\nabla \cdot \mathbf{F}$. The FT is handled by the Fast Fourier Transform algorithm. The problem of dividing by zero in the fraction when $\xi = \eta = 0$ can be excluded by simply considering the FT at that point to be equal to zero. This is motivated by the fact that the contribution of the zero frequencies consists of adding a constant to the inverse FT which does not affect the phase of the solution.

3.2. Inversion of linear system (LS)

The second method consists of writing the Laplace operator Δ from equation (10) by approximating the derivatives using finite differences e.g.

$$\partial_x^2 \phi(z_i, x_i) \approx \frac{\phi(z_i, x_{i+1}) - 2\phi(z_i, x_i) + \phi(z_i, x_{i-1})}{\Delta x^2}. \tag{17}$$

This way the ∂_x^2 and ∂_z^2 operators become tridiagonal matrices

$$M_x = \frac{1}{\Delta x^2}\begin{pmatrix} -2 & 1 & 0 & 0 & \cdots & 0 & 0 & 0 \\ 1 & -2 & 1 & 0 & \cdots & 0 & 0 & 0 \\ \vdots & \vdots & \vdots & \vdots & \ddots & \vdots & \vdots & \vdots \\ 0 & 0 & 0 & 0 & \cdots & 1 & -2 & 1 \\ 0 & 0 & 0 & 0 & \cdots & 0 & 1 & -2 \end{pmatrix} \tag{18}$$

$$M_z = \frac{1}{\Delta z^2}\begin{pmatrix} -2 & 1 & 0 & 0 & \cdots & 0 & 0 & 0 \\ 1 & -2 & 1 & 0 & \cdots & 0 & 0 & 0 \\ \vdots & \vdots & \vdots & \vdots & \ddots & \vdots & \vdots & \vdots \\ 0 & 0 & 0 & 0 & \cdots & 1 & -2 & 1 \\ 0 & 0 & 0 & 0 & \cdots & 0 & 1 & -2 \end{pmatrix} \tag{19}$$

that can be used to compute the matrix for the Laplace operator Δ as

$$\Delta = M_z \otimes I + I \otimes M_x \tag{20}$$

where $\otimes$ is the Kronecker product and I is the identity matrix. Using (20) transforms the PDE (10) into a system of linear equations which can be solved for ϕ.

4. **Numerical validation**

The retrieval in this section has been achieved following the diagram from figure 2. Simulated amplitude data is used to compute $\nabla\phi = \mathbf{F}$ using eq. (12) using finite differences and some given numeric parameters. Next $\Delta\phi$ is computed and the two solving procedures FT and LS are applied. The results are analyzed using a cross-correlation based method. A correction to the retrieved phase is applied on the cases that do not have a background.

The numeric parameters used for the simulations are $\Delta x = 2\mu m$, $\Delta z = 0.1mm$, a spatial grid (z, x) with shape 800×2400 pixels respectively, following a crop along the x axis to keep data only from the center in-between pixels 800 and 1600.

The retrieved phase is compared using the following approach. The retrieved phase is applied to the amplitude data in order to generate the reconstructed beam $\psi_{retrieved}$, which will be compared with the original numeric solution of the propagation equation $\psi_{numeric}$. First the discrete beams are normalized with the L^2 norm

$$\psi_{numeric} \to \frac{\psi_{numeric}}{\sqrt{\sum_{n,m} |\psi_{numeric}[n,m]|^2}}$$

$$\psi_{retrieved} \to \frac{\psi_{retrieved}}{\sqrt{\sum_{n,m} |\psi_{retrieved}[n,m]|^2}}$$

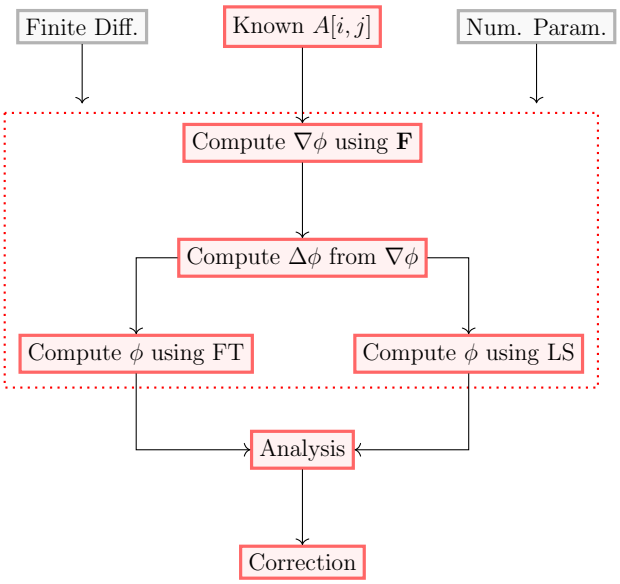

FIG. 2. Flow charts for the numeric phase retrieval.

and then their cross-correlation is computed using formula

$$(\psi_{numeric} \star \psi_{retrieved})[l,k] = \sum_{n,m} \psi_{numeric}[n,m]\psi^*_{retrieved}[n+l,m+k] \qquad (21)$$

The ideal match between two functions corresponds to a peak of the cross-correlation absolute value of 1 when the shifts between the two functions are $l = 0, k = 0$.

We have tested the method on numerically generated amplitude profiles corresponding to a superposition of three Gaussian beams, an Airy beam, and the interference of two Gaussian beams. Out of all the cases, we present in greater detail only the later since it encompasses all the aspects that are relevant to the previously discussed theoretical aspects. The initial conditions used for computing the numerical data in each case that has been used for the retrieval are plotted in figure 3.

4.1. Interference pattern with background

For the numeric validation we have used the numerically simulated interference of two Gaussian beams with initial condition

$$\psi_0(x) = \frac{1}{\sigma\sqrt{2\pi}}\left[\exp\left(-\frac{(x-\mu)^2}{2\sigma^2}\right) + \exp\left(-\frac{(x+\mu)^2}{2\sigma^2}\right)\right] + c$$

with $\sigma = 10\mu m$, $\mu = 0.2mm$ (figure 3.A) and background of $c = 100a.u.$. The width of each Gaussian beam has been chosen via the σ parameter in order to generate a spread beam after a short propagation distance, which was required in order to obtain the interference, without introducing numerical artifacts due to the step on the transverse domain. The numerical solution for this initial

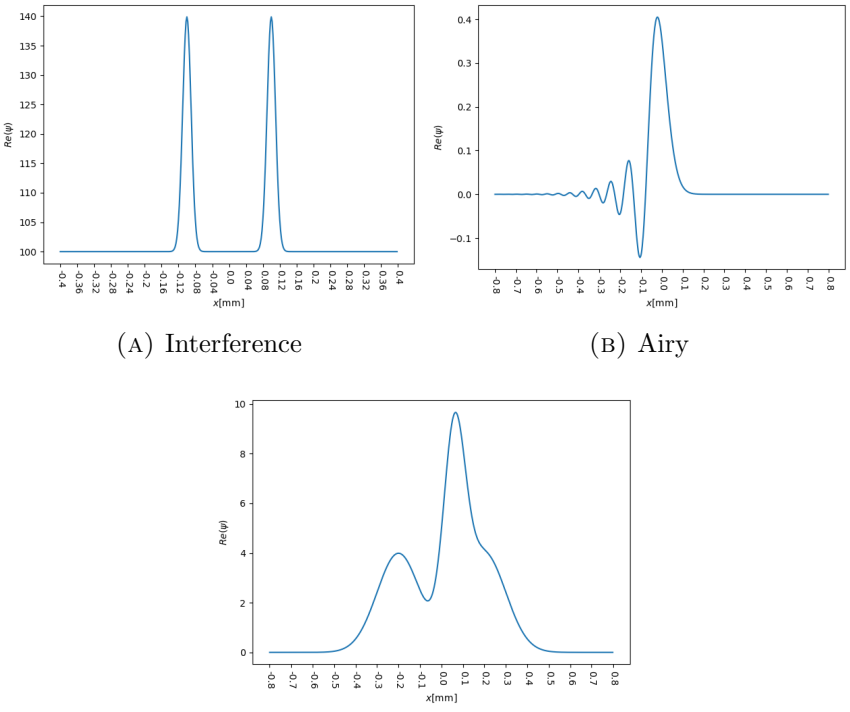

(A) Interference

(B) Airy

(C) Gaussian superposition

FIG. 3. Initial conditions used for the computation of the numerical data used in testing the method.

conditions has been computed in order to generate the amplitude data from figure 4.A which will be used in the following to test WBPR. The phase of the solution (figure 4.B) is used for comparison with the retrieved phase from WBPR.

For the comparison with the initial phase function, the retrieved one is processed using

$$\phi_{FT} := \arg(|\psi + c| \exp(i\phi_{FT}) - c)$$

and ϕ_{LS} similarly for the LS method, where ψ is the computed numerical solution for the interference pattern. The cross-correlation comparison using the reconstructed complex functions $\psi_{FT} = |\psi| \exp(i\phi_{FT})$ and $\psi_{LS} = |\psi| \exp(i\phi_{LS})$ returns non-shifted peaks of 0.988 for FT and 0.995 for LS which indicates the similitude between the reference and the reconstructed beams.

4.2. Interference pattern without background

Here we use the interference pattern from subsection 4.1 with the implicit exception of not adding the background for the retrieval. During the numerical computation of the term $\nabla \cdot \mathbf{F}$ a threshold criterion is introduced by setting the

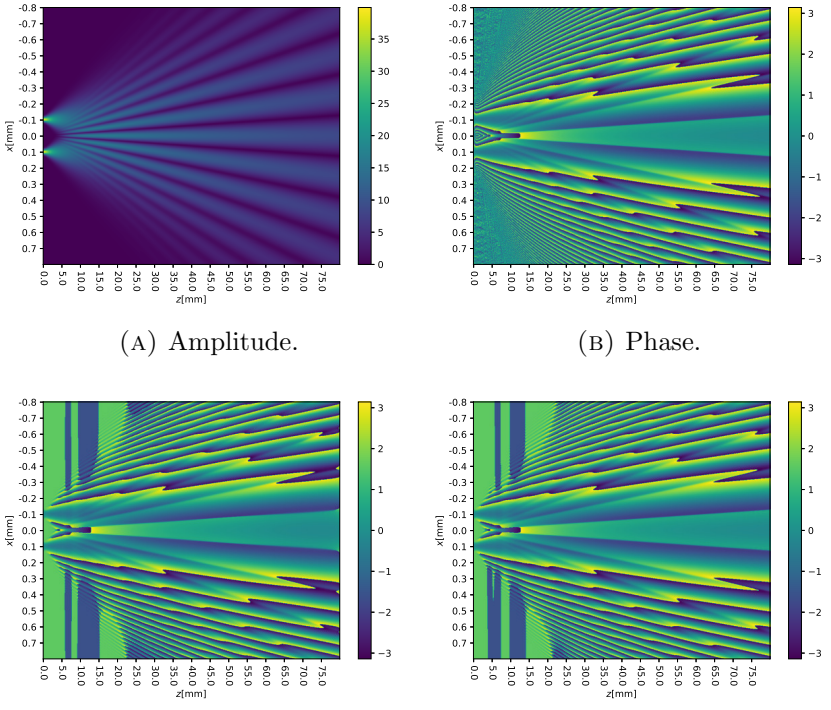

(A) Amplitude. (B) Phase.

(C) FT method. (D) LS method.

FIG. 4. Results of computing the phase for the amplitude functions of the interference given by two Gaussian beams using the FT and LS methods.

amplitude function to zero whenever its values are less than 1% of the global peak.

The retrieved phase functions have a piston term $\phi_0(z)$[12] that varies along the propagation axis as it can be seen in figure 5. Due to the piston term, by comparing cases 4.C and 4.D to 5.A and 5.B respectively it can be easily noticed that the retrieved phases are different. Other differences between the reference phase and the retrieved one include the existence of slow varying terms. The most common types are linear and quadratic, which have the effect of tilting the propagation direction of the beam, and adding a lens effect respectively.

In order to correct for the existence of the piston and slow varying terms the following correction has been applied on both FT and LS methods. The retrieved phase is applied to the input amplitude data, generating an intermediary beam function. The intermediary beam function consists of multiple equally spaced complex profiles. Each such profile is used to compute a reconstructed beam by forward and backward propagating it until the entire propagation domain is covered. The amplitude of the reconstructed beam is

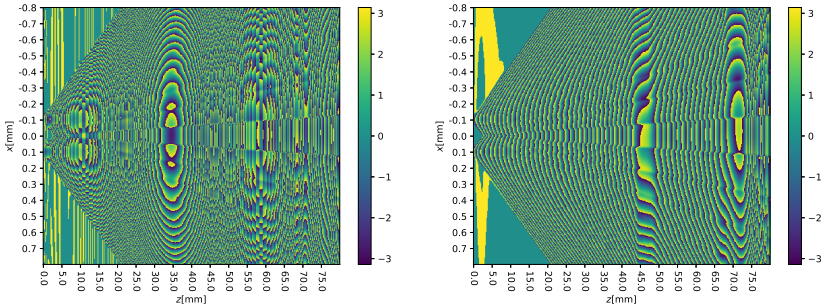

(A) Phase FT. (B) Phase LS.

FIG. 5. The phase functions retrieved for the interference pattern without background.

compared with the initial amplitude data using cross-correlation as in the previous case. The maximum value of the cross-correlation for each reconstructed beam is stored in order to identify the best reconstructed beam.

For both FT and LS methods during this example, the non-shifted cross-correlation amplitude peaks range from 0.74 and 0.9994 for all the reconstructed beams, with the best reconstructed beams having values of 0.9994 for LS and 0.9993 for FT. For a visual comparison, the phases of the best reconstructed cases are shown in figure 6. It should be mentioned that the visible differences between figure 6 compared with figure 4 are due to a global phase constant.

5. **Further discussions**

The two cases that have been presented, although treated differently in terms of the existence of background, address the same problem regarding the phase retrieval. The background case has the advantage of not requiring to know the initial condition. The case without background ignores the initial condition term, but requires additional corrections because of it. Both methods can then be regarded as trying to eliminate the existence of either piston or slow varying terms.

In the case of having a background, the piston term is corrected due to not having the influence of the initial condition term near the boundary of the transverse domain. The slowly varying terms can still appear due to the numerical implementation of the retrieval, which in turn can be corrected following the same procedure as for the case with background. For the case of having a background, the correction is necessary since the piston term can appear due to ignoring the initial condition term. The slow varying terms are avoided by searching for the profile that best reconstructs the amplitude profile. Thus from a computational perspective, the background case is faster

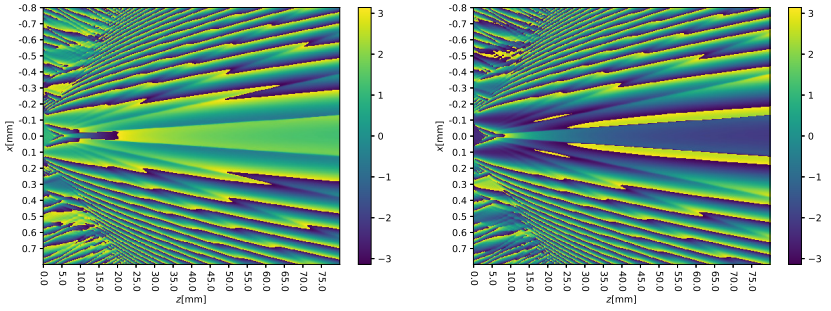

(A) Phase FT. (B) Phase LS.

FIG. 6. Results of computing the reconstructed amplitude and phase functions from amplitude data without background.

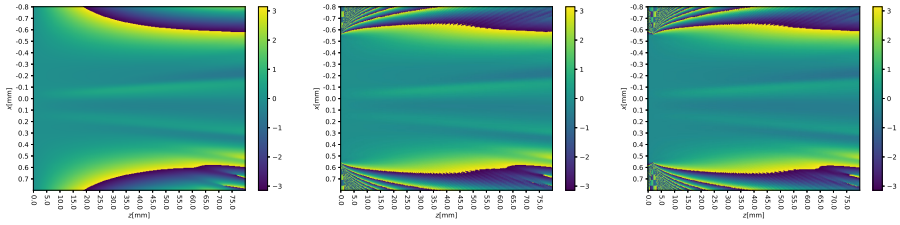

(A) Phase (B) LS (C) FT

FIG. 7. Phase (left) and retrieved phases with LS (center) and FT (right) for a Gaussian superposition beam.

but less general, while the no background case is slower due to the required correction but is more general.

In order to apply the method, amplitude data can be acquired from intensity measurements using a basic CCD camera at equally spaced intervals along the propagation axis. Since the method is only 1-dimensional in the transverse plane, the cases that can be investigated must be ideally constant along one transverse axis, which usually is the case for interference. Due to the use of ca camera that records the images in a digital format, the intensity values are discrete due to recording the intensity levels using a given number of bits, usually 8. Thus, the introduction of the threshold value from the case without background is motivated by the discrete nature of the recorded images.

As mentioned previously, the phase retrieval method has also been tested on other scenarios. The results are presented in figure 7 for Gaussian superposition beam with background with 0.99 values for both LS and FT, and figure 8 for Airy beam without background with 0.98 for LS and 0.99 for FT.

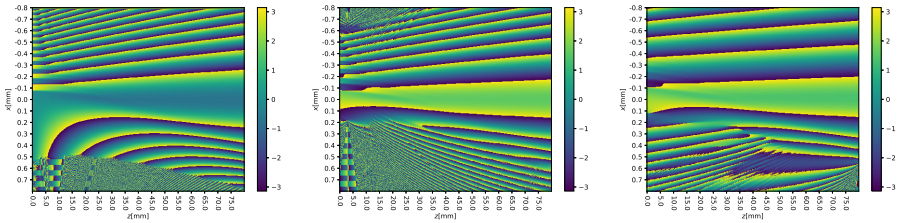

(A) Phase (B) LS (C) FT

FIG. 8. Phase (left) and retrieved phases with LS (center) and FT (right) for an Airy beam without background.

6. Conclusion

A method of computing the phase function from the amplitude of a 1-dimensional transverse optical beam for a finite propagation interval has been presented. The method is applied on amplitude data with and without background, with an additional correction being applied on the later case. The results indicate that the method can be applied on amplitude data that contain points where the amplitude is zero although the computation time is increased.

APPENDIX

Solving equation (3)

Equation (3) can be identified with a non-homogeneous first order differential equation with variable coefficients

$$A\partial_x^2\phi + 2\partial_x A\partial_x\phi = -2k\partial_z A \tag{22}$$

where the variable is $\partial_x\phi$. For solving (22) we use multiply equation (22) by A which gives

$$A^2\partial_x^2\phi + 2A\partial_x A\partial_x\phi = -2kA\partial_z A \tag{23}$$

which can be written as

$$\partial_x(A^2\partial_x\phi) = -k\partial_z A^2. \tag{24}$$

Integrating equation (24) by $\int_0^x dx'$ gives

$$A^2\partial_x\phi = -k\int_0^x \partial_z A^2 dx' \tag{25}$$

which gives the solution for $\partial_x\phi$ as

$$\partial_x\phi = -\frac{k}{A^2}\int_0^x \partial_z A^2 dx' + \frac{(A^2\partial_x\phi)|_{x=0}}{A^2} \tag{26}$$

Deriving equation (16)

Equation (16) can be derived by using the property of the Fourier Transform

$$\mathscr{F}[\partial_x f(x)] = 2\pi i\xi \mathscr{F}[f(x)] \tag{27}$$

where ξ is the frequency associated with the x variable. Equation (16) is derived from equation (10)

$$\Delta\phi = \partial_x^2\phi + \partial_z^2\phi = \nabla \cdot \mathbf{F} \tag{28}$$

on which the Fourier Transform is applied

$$\mathscr{F}[\partial_x^2\phi + \partial_z^2\phi] = \mathscr{F}[\nabla \cdot \mathbf{F}]. \tag{29}$$

Each derivative in the left-hand side of equation (31) becomes

$$-(4\pi^2\xi^2 + 4\pi^2\eta^2)\tilde{\phi} = \mathscr{F}[\nabla \cdot \mathbf{F}] \tag{30}$$

according to equation (27), where $\mathscr{F}[\phi] = \tilde{\phi}$, and η is the frequency associated with the z variable. By rewriting equation (30) we get

$$\tilde{\phi} = -\frac{1}{4\pi^2(\xi^2 + \eta^2)}\mathscr{F}[\nabla \cdot \mathbf{F}] \tag{31}$$

which is the same as equation (16).

REFERENCES

[1] *L. Taylor*, The phase retrieval problem, IEEE Transactions on Antennas and Propagation, **29**(1981), No. 2, 386-391.

[2] *R.W. Gerchberg*, Phase determination for image and diffraction plane pictures in the electron microscope, Optik (Stuttgart), **34**(1971), 275.

[3] *J.R. Fienup*, Phase retrieval algorithms: a comparison, Applied optics, **21**(1982), No. 15, 2758-2769.

[4] *J.W. Wood, M.A. Fiddy, R.E. Burge*, Phase retrieval using two intensity measurements in the complex plane, Optics letters, **6**(1981), No. 11, 514-516.

[5] *L. Bruel*, Numerical phase retrieval from beam intensity measurements in three planes, InLaser-Induced Damage in Optical Materials: 2002 and 7th International Workshop on Laser Beam and Optics Characterization, International Society for Optics and Photonics, **4932**, 590-598.

[6] *V.Y. Zavalova, A.V. Kudryashov*, Shack-Hartmann wavefront sensor for laser beam analyses, InHigh-Resolution Wavefront Control: Methods, Devices, and Applications III, International Society for Optics and Photonics, **4493**(2002), 277-284.

[7] *A. Polo, V. Kutchoukov, F. Bociort, S.F. Pereira, H.P. Urbach*, Determination of wavefront structure for a Hartmann wavefront sensor using a phase-retrieval method, Optics express, **20**(2012), No. 7, 7822-7832.

[8] *C. Li, B. Li, S. Zhang*, Phase retrieval using a modified Shack–Hartmann wavefront sensor with defocus, Applied optics, **53**(2014), No. 4, 618-624.

[9] *L. Loetgering, H. Froese, T. Wilhein, M. Rose*, Phase retrieval via propagation-based interferometry, Physical Review A, **95**(2017), No. 3, 033819.

[10] *G. Pedrini, D. Claus*, Phase retrieval using bidirectional interference, Applied Optics, **60**(2021), No. 12, 3517-3525.

[11] *N. Nakajima*, Noniterative phase retrieval from a single diffraction intensity pattern by use of an aperture array, Physical review letters, **98**(2007), No. 22, 223901.

[12] *M.R. Teague*, Image formation in terms of the transport equation. JOSA A. **2**(1985), No. 11, 2019-26.

[13] *M.R. Teague*, Deterministic phase retrieval: a Green's function solution, JOSA, **73**(1983), No. 11, 1434-1441.

[14] *T.E. Gureyev, A. Roberts, K.A. Nugent*, Phase retrieval with the transport-of-intensity equation: matrix solution with use of Zernike polynomials, JOSA A, **12**(1995), No. 9, 1932-41.

[15] *T.E. Gureyev, K.A. Nugent*, Phase retrieval with the transport-of-intensity equation, II. Orthogonal series solution for nonuniform illumination, JOSA A, **13**(1996), No. 8, 1670-82.

[16] *J. Frank, S. Altmeyer, G. Wernicke*, Non-interferometric, non-iterative phase retrieval by Green's functions, JOSA A, **27**(2010), No. 10, 2244-2251.

[17] *C. Zuo, J. Li, J. Sun, Y. Fan, J. Zhang, L. Lu, R. Zhang, B. Wang, L. Huang, Q. Chen*, Transport of intensity equation: a tutorial. Optics and Lasers in Engineering. **135**(2020), 106187.

[18] *D. Paganin, K.A. Nugent*, Noninterferometric phase imaging with partially coherent light. Physical review letters. **80**(1998), No. 12, 2586.

[19] *A. Couairon, E. Brambilla, T. Corti, D. Majus, O. de J. Ramírez-Góngora, and M. Kolesik*, Practitioner's guide to laser pulse propagation models and simulation, The European Physical Journal Special Topics **199**(2011), No. 1, 5-76.